Hollow core-shell structured $Cu_2O@Cu_{1.8}S$ spheres as novel electrode for non-enzymatic glucose sensing

Miaomiao Cao[1], Hui Wang[1], Shan Ji[2], Qian Zhao[1], Bruno G. Pollet [3] and

Rongfang Wang[1]

[1] Institute of Chemical Engineering, Qingdao University of Science and Technology, Qingdao, 266042, China

[2] College of Biological, Chemical Science and Chemical Engineering, Jiaxing University, Jiaxing, 314001, China

[3] Department of Energy and Process Engineering, Faculty of Engineering, Norwegian University of Science and Technology (NTNU), NO-7491 Trondheim, Norway

Corresponding authors:

Shan Ji (*): jissshan@126.com, Tel./fax: +86 (0)15024355548

Rongfang Wang (**): wrf38745779@126.com, Tel./fax: +86 (0)13919839172

Abstract

This study reports a novel hollow $Cu_2O@Cu_{1.8}S$ material used as an electrode for non-enzymatic glucose sensing. $Cu_2O@Cu_{1.8}S$ was successfully synthesized by a facile in-situ growth method. The obtained $Cu_2O@Cu_{1.8}S$ exhibited a hollow structure with a $Cu_{1.8}S$ rich surface. Electrochemical results revealed that the $Cu_2O@Cu_{1.8}S$ electrode exhibited a much higher electrocatalytic activity toward glucose oxidation

than Cu_2O spheres owing to the synergistic effect between Cu_2O and $Cu_{1.8}S$. The $Cu_2O@Cu_{1.8}S$ based sensor showed a rapid sensing response of 5 s, a wide linear range in concentrations of 1–1,000 µM, a high sensitivity of 3,630 $\mu A \cdot mM^{-1}cm^{-2}$, and a low detection limit of 0.0678 µM, along with an excellent selectivity, thus leading to a promising candidate for non-enzymatic glucose detection.

Keywords: Copper sulfide; Copper oxide; Hollow structure; Glucose; Non-enzymatic sensor

1. Introduction

Considerable efforts have been devoted to the development of fast, reliable and simple methods for monitoring glucose in the fields of clinical diagnostics, food industry and biotechnology [1]. The first enzyme glucose biosensor was reported in 1962 [2], and since then, glucose oxidase has attracted much research interest in the development of enzyme glucose biosensors due to its high sensitivity and activity [3-5]. Unfortunately, due to the high cost, complicated immobilization procedure, the glucose oxidase instability and poor reproducibility (as the catalytic activity can be easily affected by, for example, pH, temperature and humidity), extensive efforts have focused on the development of non-enzymatic glucose sensors to replace glucose oxidase biosensors [4, 6, 7]. Among these non-enzymatic glucose sensors, electrochemical non-enzymatic glucose sensors are attractive due to their low cost, high efficiency and ease of operation. Various non-enzymatic electrode materials, such as noble metal [8, 9], metal oxides [10, 11], metal sulfide and their hybrids [12, 13], have been widely developed for glucose detection.

2

It is well-known that copper oxide is a *p*-type semi-conductor material with great potential for use as a non-enzymatic sensor for detecting glucose due to its low cost, environmental friendliness and high catalytic activity [14-18]. However, copper oxides cannot be used as non-invasive glucose detection in saliva for routine glucose monitoring because of their poor linear detection range [19, 20]. In order to improve the detection ability, intensive R&D efforts have been devoted to combine copper oxide nanoparticles with other materials, such as metal, carbon materials and metal oxides [19, 21-24]. It has been reported that the fast response, low detection limit and excellent sensitivity for glucose detection can be achieved by combining copper oxides with other materials, because the combination can significantly improve electrical conductivity or/and synergistic effect. Thus, developing copper oxide hybrid materials can be an effective way to improve detection performance.

Copper sulfide possesses a variety of crystal polymorphs and structures. Among these copper sulfides, Cu_2S and CuS have been developed as non-enzymatic glucose sensors, which show fast response, low detection limit and good sensitivity for glucose detection. Thus, it is expected that the highly sensitive detection of non-enzymatic glucose sensor could be achieved by forming hybrid structures which comprise copper oxide and copper sulfide. A literature search revealed that there is no report demonstrating the use of hybrid copper sulfide as sensors for glucose detection. In this study, a facile method was developed to synthesize hollow $Cu_2O@Cu_{1.8}S$ spheres with $Cu_{1.8}S$ rich surface via an in-situ growth method. The results indicated

that the as-prepared samples exhibited a much better performance for glucose detection in terms of sensitivity, detection range and selectivity than Cu_2O.

2. Experimental

2.1 Preparation of $Cu_2O@Cu_{1.8}S$

All chemicals used throughout the experiments were of analytical grade (AR) and used without further purification. The first step of preparation of $Cu_2O@Cu_{1.8}S$ was to synthesize Cu_2O; the detailed procedure is as follows: 0.3993g of $(CH_3COO)_2Cu \cdot H_2O$ were firstly dissolved in 25 ml of DMF containing 0.3 ml deionized water and magnetically stirred for 10 min, then ultrasonically treated for 3 min. After that, the solution was stirred at 85 ℃ for 10 min and then left at room temperature for 2 h. The obtained product was washed thoroughly with ethanol (95%), collected by centrifuge and dried in a vacuum oven for 12 h at 40℃. Subsequently, the obtained Cu_2O nanospheres (25 mg) were added into 15 ml of ultrapure water and ultrasonically treated for 5 min. The Cu_2O solution was introduced into a Na_2S solution ($Na_2S \cdot 9H_2O$ was dissolved into 10 ml distilled water, and a molar ratio of $Na_2S \cdot 9H_2O$:CuO was 1.5:1), and then treated in an ice cooled ultrasonic bath for 5 min. A black product was formed during the ultrasonic treatment. The obtained black product was washed with 95% ethanol, collected by centrifuge and then dried in a vacuum oven at 40 ℃ for 12 h. The final product was labelled as $Cu_2O@Cu_{1.8}S$.

2.2 Characterization

The crystalline structures of the samples were analyzed using X-ray diffraction (XRD, Shimadzu XD-3A (Japan) goniometer, using CuKα radiation operated at 40 kV and 35 mA). The morphology of the catalysts was observed by a Carl Zeiss Ultra Plus field emission scanning electron microscopy (SEM) and transmission electron microscopy (TEM) measurement which was carried out using a JEM-2010 Electron Microscope (Japan) with an acceleration voltage of 200 kV. Spectroscopy (XPS) tests were performed on a PHI-5702 (American). Binding energies were calibrated by referencing to the C1s peak at 285.0 eV.

2.3 Electrochemical measurements

Electrochemical measurements were carried out on an electrochemical work station (CHI 650D). A conventional three-electrode electrochemical cell was used comprising of a platinum wire as counter electrode, an Ag/AgCl (saturated KCl solution) as reference electrode, and a working electrode made of a thin film catalyst layer mounted on a 5-mm diameter glassy carbon disc (rotating disc electrode – *rde*). The thin film was prepared as follows: 2 mg of catalyst were dispersed ultrasonically in a 0.4 mL of Nafion®/ethanol solution (25 wt.% Nafion®). 8 μL of the above solution was transferred onto the glassy carbon and then dried in air. Cyclic voltammetry (CV) measurement was carried out in a three-electrode system using 0.1 M NaOH aqueous solution as electrolyte. The potential scan rate was 50 mV s^{-1} in the potential range 0.20 - 0.80 V *vs*. Ag/AgCl. The electrode was firstly scanned in NaOH in the absence of glucose, subsequently scanned in NaOH with 50 μM, 100 μM, 500

µM, 1 mM, 2 mM, 3 mM, 4 mM and 5 mM of glucose respectively. Amperometric responses of the as-prepared electrodes with increasing glucose concentration was carried out in a 0.1 M NaOH solution and the rotation speed of the *rde* was set at 1,000 rpm. The selectivity of the electrodes was firstly tested in 0.1 M NaOH with 1,000 µM of glucose and then 0.1 mM of ascorbic acid (AA), uric acid (UA), NaCl and L-glucose was introduced into the NaOH/glucose solution respectively.
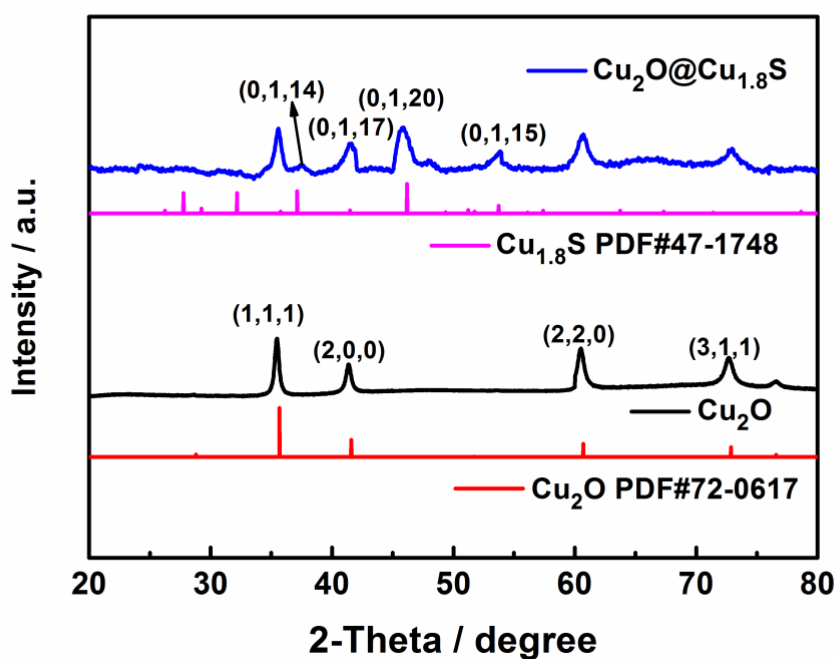
3. Results and discussion

Figure 1. XRD patterns of the Cu_2O and $Cu_2O@Cu_{1.8}S$ samples.

Figure 1 shows the XRD patterns of Cu_2O and $Cu_2O@Cu_{1.8}S$. In the case of Cu_2O, the diffraction peaks appear at $2\theta = 35.4$, 41.5, 60.5, 72.7 and 76.6°, corresponding to (110), (111), (200), (220), and (311) crystal planes of cubic Cu_2O (PDF#72-0617), respectively. No diffraction peak of CuO was found, indicating that only a single

phase Cu_2O was obtained. In the XRD pattern of $Cu_2O@Cu_{1.8}S$, beside the diffraction peaks of Cu_2O, four obvious diffraction peaks at 2θ degree of 37.6 45.8, 48.0 and 54.0° were observed. By carefully analyzing the data and critically reviewing the previous database, these diffraction peaks can be indexed as (0114), (0117), (0120), and (1115) planes of rhombohedral $Cu_{1.8}S$ (JCPDS No. 47-1748). The results indicated that $Cu_2O@Cu_{1.8}S$ exhibited heterogeneous crystal structures.

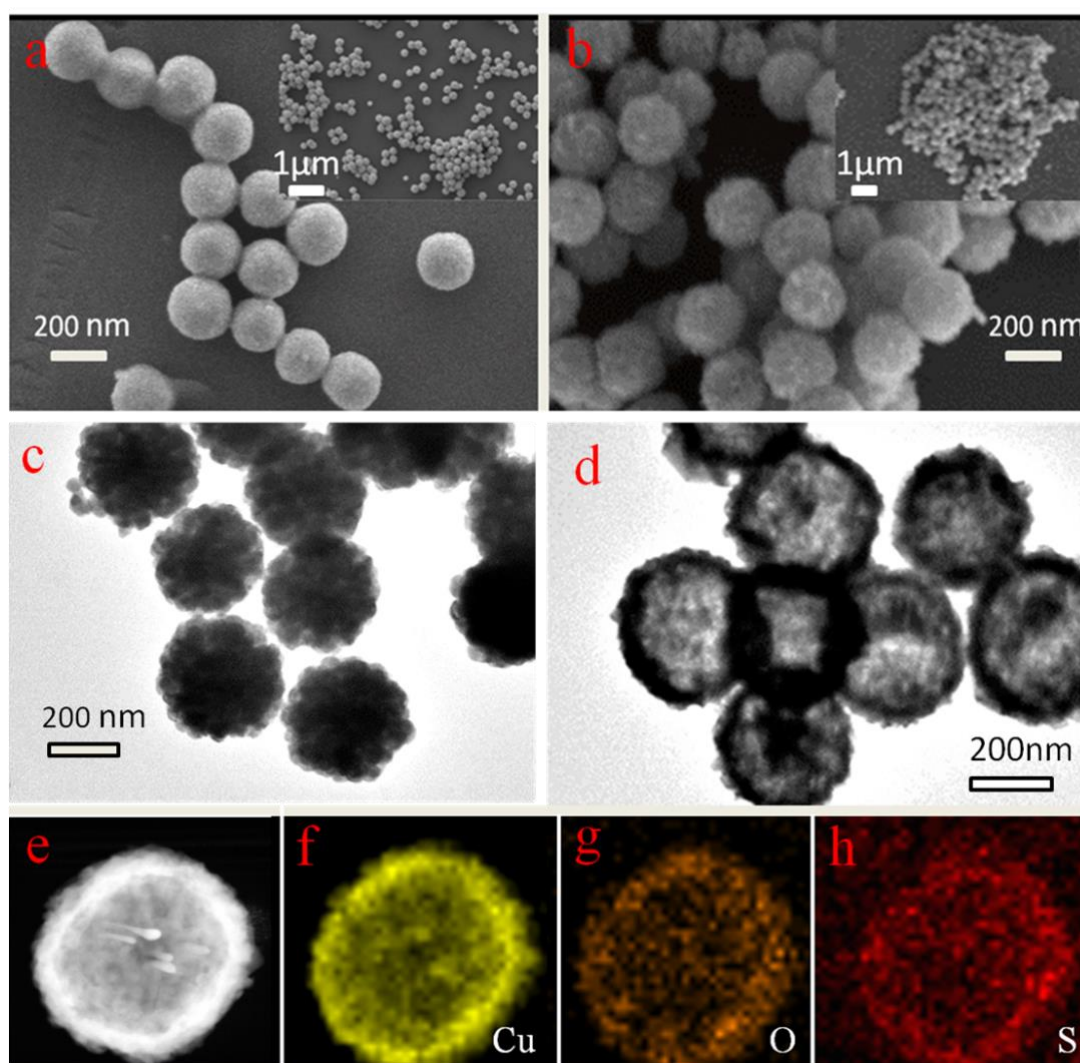**Figure 2.** SEM and TEM images and of the Cu_2O (a,c) and $Cu_2O@Cu_{1.8}S$ (b,d); STEM (e) and corresponding EELS element maps (f-h) of $Cu_2O@Cu_{1.8}S$.

The morphology of the as-prepared samples was studied by SEM and TEM. Figure

7

2(a) shows the overall morphology of the samples composed of large-scale uniform, sphere-like architectures of ca. 300 nm in diameter. After the in-situ formation of $Cu_2O@Cu_{1.8}S$, the sphere shape was retained and the diameter increased to ca. 350 nm (Fig. 2(b)). The detail structure was investigated by TEM (Fig. 2(c)). The TEM image of $Cu_2O@Cu_{1.8}S$ clearly shows that the Cu_2O spheres was made up of small particles. TEM images of $Cu_2O@Cu_{1.8}S$, as represented in Figure 2(d), shows a hollow sphere-like structure assembled by small particles. According to He and Zhu *et al.*[25, 26]，the formation of $Cu_{1.8}S$ could be ascribed to the exchange reaction between S^{2-} and oxygen anions. Moreover, the mobility of oxygen anions was faster than that of the sulfur, leading to a continuous mass relocation of Cu_2O crystallites from the inside out during the formation of $Cu_{1.8}S$ with a continuous supply of S^{2-} for the exchange reaction, resulting in the hollow structure of $Cu_2O@Cu_{1.8}S$. Elemental distribution in $Cu_2O@Cu_{1.8}S$ was evaluated by HAADF-STEM (Fig. 2(e)) and corresponding EELS element concentration maps (Fig. 2(f-h)). Comparing the STEM and the elemental maps, the formation of a hollow structure is again confirmed. Moreover, the slight increase in the S diameter compared to that of O suggests the formation of $Cu_{1.8}S$-rich surface.
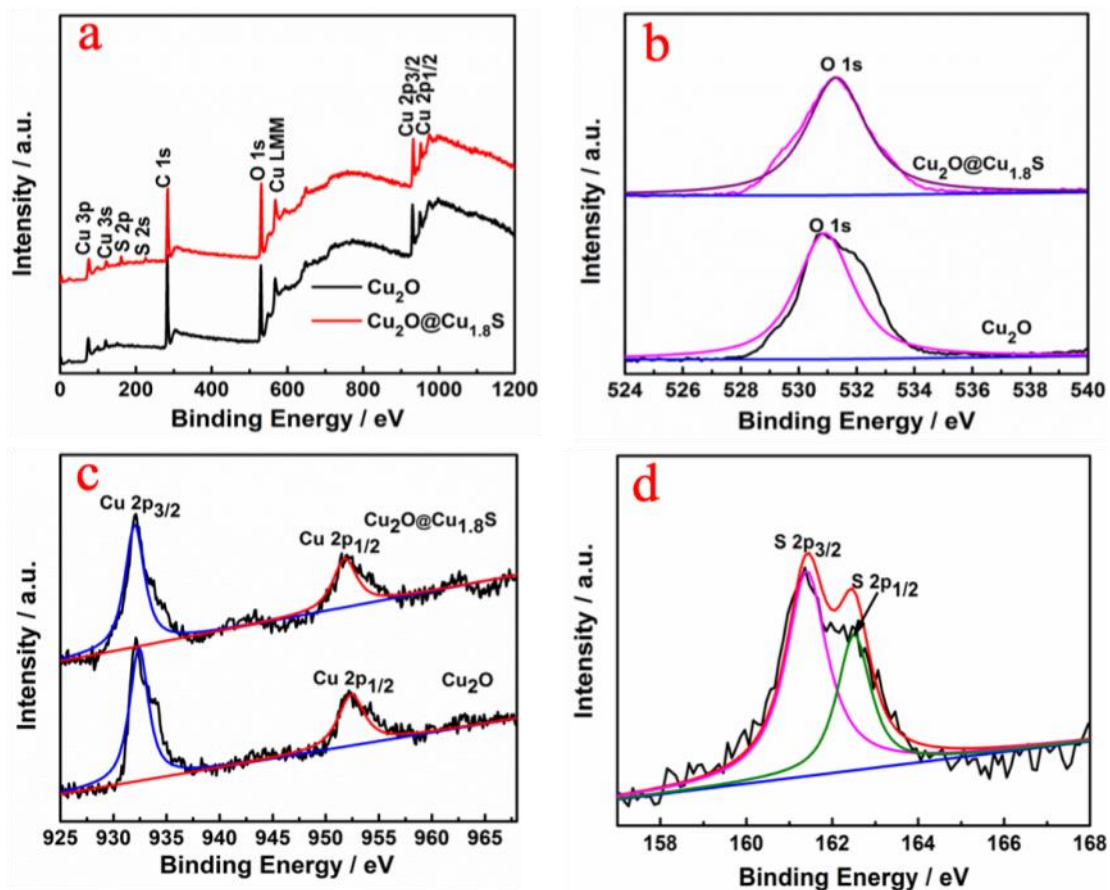
Figure 3. (a) XPS survey spectra of Cu_2O and $Cu_2O@Cu_{1.8}S$; (b) XPS spectra of Cu

2p region in Cu_2O and $Cu_2O@Cu_{1.8}S$; (c) XPS spectra of O 1s region in Cu_2O and

$Cu_2O@Cu_{1.8}S$; (d) XPS spectra of S2p region in Cu_2O and $Cu_2O@Cu_{1.8}S$ dendrite

XPS analyses were conducted to further investigate the chemical state and

electronic state of the elements in Cu_2O and $Cu_2O@Cu_{1.8}S$. A survey scan (Fig. 3(a))

indicates the presence of Cu and O in Cu_2O and $Cu_2O@Cu_{1.8}S$, and the additional S

signals in $Cu_2O@Cu_{1.8}S$. The detailed element contents were determined from XPS

analyses. They revealed that the atomic ratio of Cu to O was 1.95:1 for Cu_2O, close to

2, suggesting the formation of Cu_2O, a finding which is in good agreement with the

XRD results. In the case of $Cu_2O@Cu_{1.8}S$, the S content was ca. 22.7 at.%. After

calculation, the molar ratio of Cu_2O to $Cu_{1.8}S$ was found to be 1:2. Furthermore, as shown in Figure 3(b), the Cu $2p$ peak of Cu_2O can be split into Cu $2p3/2$ at 932.4 eV and Cu $2p1/2$ at 952.4 eV, which is approximately consistent with the peak positions of Cu $2p$ spectra of reference Cu_2O [27], further confirming the formation of Cu_2O. A more detailed analysis in the spectra (Fig. 3(b)) indicates a slight shift to lower energy for Cu $2p3/2$ (932.0 eV) and Cu $2p1/2$ (951.8 eV) peaks of $Cu_{1.8}S$ compared to those of Cu_2O, which are in good agreement with values found in the literature [28, 29]. It was also found that a shift in binding energy occurred as shown in the O $1s$ spectra (Fig. 3(c)); i.e. a binding energy of O $1s$ positively shifted from 530.9 eV in Cu_2O to 531.3 eV in $Cu_2O@Cu_{1.8}S$, indicating the presence of S [28, 29]. In addition, the S $2p$ peak can be split into two doublets centered at 161.4 and 162.5 eV, corresponding to the sulfides of the multivalent copper [29].
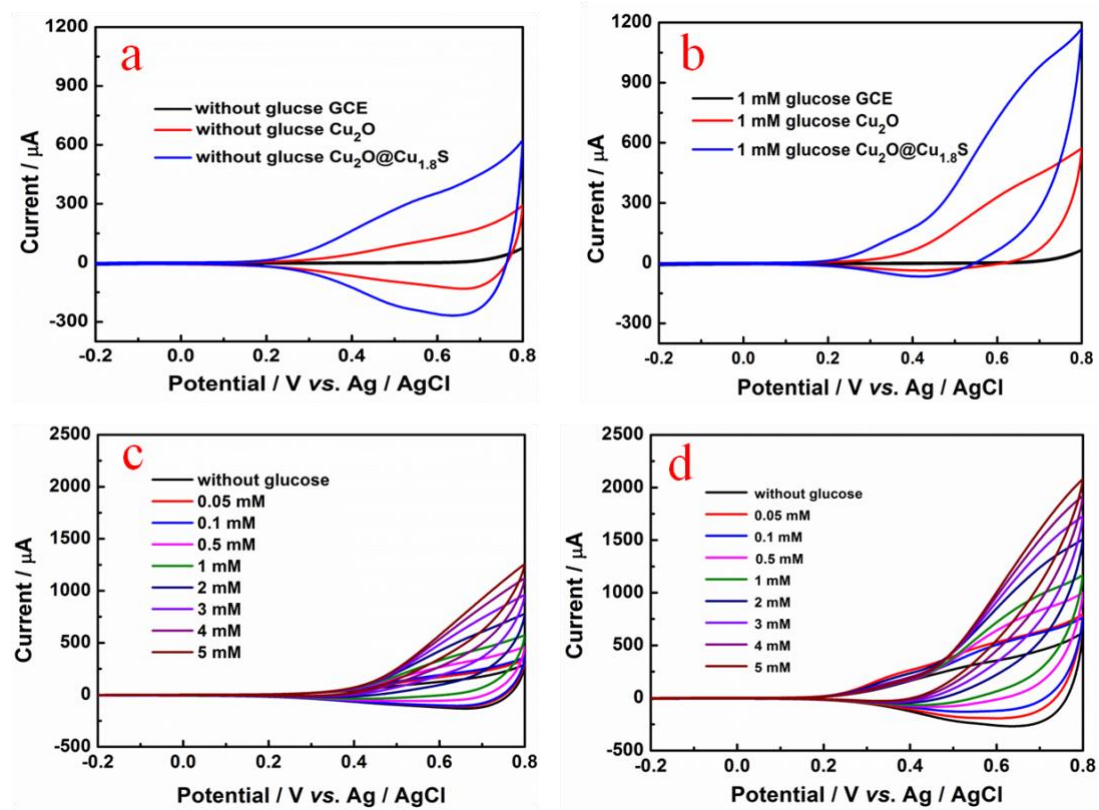
Figure 4. CV curves of Cu_2O and $Cu_2O@Cu_{1.8}S$ in 0.1 M NaOH (a) and 0.1 M NaOH +

0.1 mM glucose solution (b) at a scan rate of 50 mV s^{-1}; CV curves of Cu_2O (c) and

$Cu_2O@Cu_{1.8}S$ (d) in 0.1 M NaOH + 0.05, 0.1, 0.5, 1, 2, 3, 4 and 5 mM glucose solution

at a scan rate of 50 mV s^{-1}.

The electrochemical behaviour of Cu_2O and $Cu_2O@Cu_{1.8}S$ was firstly investigated

by cyclic voltammetry (CV) in a 0.1 mol L^{-1} KOH solution in the absence and

presence of glucose (Fig. 4). As shown in Figure 4(a), the CVs on the glassy carbon

disc electrode does not shows any redox peaks in the working potential range. The

same observation is also found in Figure 4(b) when glucose is present, indicating that

the bare glassy carbon disc electrode is not electrochemically active toward glucose.

After Cu_2O was loaded onto the electrode and immersed in 0.1 mol L^{-1} NaOH, the CV

showed an oxidation peak in the range +0.20 to 0.80 V vs. Ag/AgCl, corresponding to

the oxidation of Cu(I); the reverse reaction (reduction back to Cu_2O) was also observed in the negative potential scan. The redox reactions can be described as follows [30-32]:

$$Cu_2O + 2OH^- \rightarrow 2CuO + H_2O + 2e^- \qquad (1)$$
$$CuO + OH^- \rightarrow CuOOH + e^- \qquad (2)$$
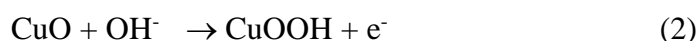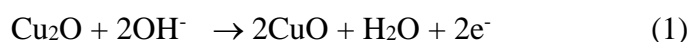
In our conditions, it is possible that the electron transfer between Cu (II) and Cu (III) could facilitate electron transfer during the oxidation of glucose. In the CVs of $Cu_2O@Cu_{1.8}S$, it can be observed that the redox peaks shift negatively compared to Cu_2O, suggesting that the electron transfer between Cu (I) and Cu (III) is easier. In the presence of glucose (Fig. 4(b)), the current increased compared to that in the absence of glucose, indicating that Cu_2O and $Cu_2O@Cu_{1.8}S$ have a catalytic activity toward glucose oxidation [33, 34]. It can also be observed that the current generated by the $Cu_2O@Cu_{1.8}S$ electrode was larger than that of Cu_2O, suggesting that the glucose oxidation occurred easily on $Cu_2O@Cu_{1.8}S$. Figure 4(c,d) shows that with increasing glucose concentration over a range of 0.05, 0.1, 0.5, 1, 2, 3, 4 and 5 mM, the activities of Cu_2O and $Cu_2O@Cu_{1.8}S$ increased linearly, indicating that specific electrocatalytic activity toward glucose oxidation had occurred. Moreover, it was found that all current responses on $Cu_2O@Cu_{1.8}S$ were larger than those obtained on Cu_2O, suggesting that $Cu_2O@Cu_{1.8}S$ has good catalytic activity for glucose oxidation compared to Cu_2O.
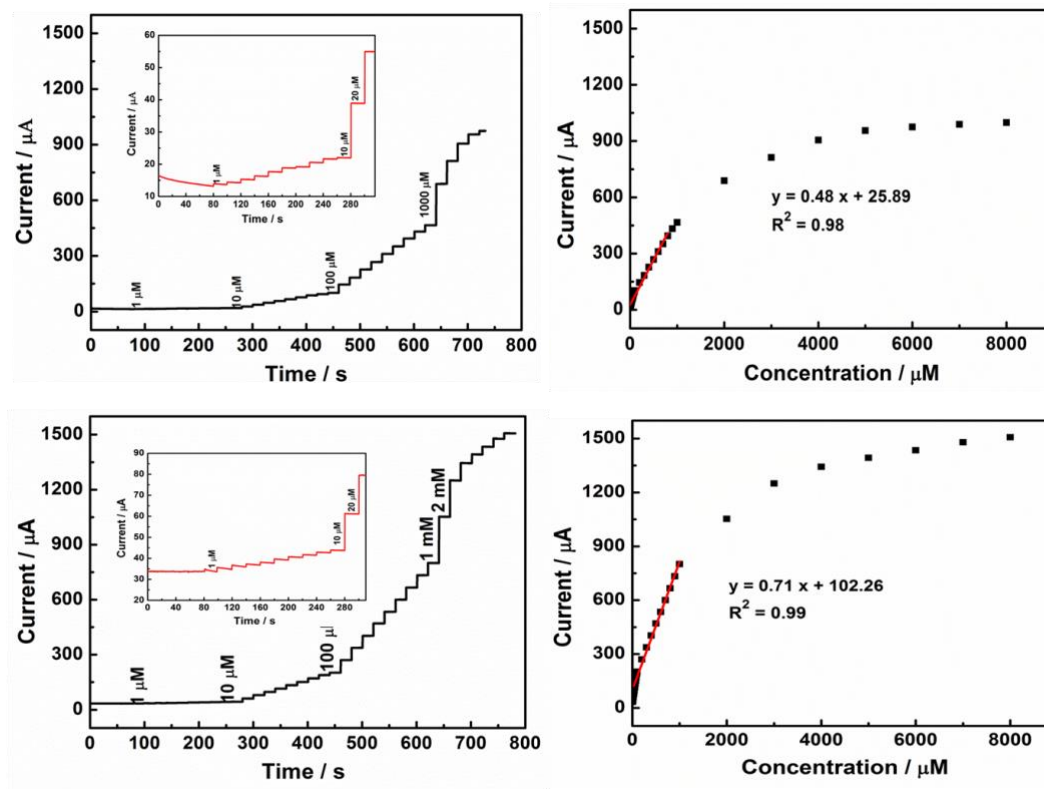
Figure 5. (a) Amperometric responses on Cu_2O and $Cu_2O@Cu_{1.8}S$ electrodes with successive addition of different amounts of glucose in 0.1 M NaOH at a potential of +0.5 V *vs.* Ag/AgCl; Insert: enlarged amperometric response of the electrode at low concentrations; (b) current–glucose concentration calibration curve obtained from Figure 4(b).

The amperometric method is a very sensitive method which can provide less signal-to-noise ratio and can result in rapid detection of an analyte. Therefore, in this study, the as-prepared $Cu_2O@Cu_{1.8}S$ and Cu_2O electrode was further used to investigate their amperometric responses at various glucose concentrations in a 0.1 M NaOH solution. Figure 5(a,c) shows the amperometric responses of $Cu_2O@Cu_{1.8}S$ and Cu_2O electrode as an enzyme-free sensor for successive additions of glucose at different concentrations under the optimized detection potential of +0.50 V vs.

Ag/AgCl. The inserts in the figure show enlarged amperometric responses at low glucose concentrations. From the figures, it can be observed that the proposed sensor reached a steady-state current (95 % of the maximum) within 20 s (Fig. 7(a), inset), demonstrating a rapid amperometric response behaviour. As expected, the $Cu_2O@Cu_{1.8}S$ displayed a stronger glucose response compared to the Cu_2O modified glassy carbon disc electrode, which can be explained by its superior electrocatalytic activities for glucose oxidation and rapid charge-transfer behavior. Figure 5(b,d) show the electrochemical response calibration curve of Cu_2O and $Cu_2O@Cu_{1.8}S$, which follows a linear response to glucose within the glucose concentration range of 0.1 to 800 mM ($R^2 = 0.98$) for Cu_2O and 0.1 to 1,000 mM ($R^2 = 0.99$) for $Cu_2O@Cu_{1.8}S$. The upper-limit of the linear range is beyond the physiological level of 3–8 mM for practical use of glucose detection. From the slope of current *vs.* glucose concentration, a sensitivity of 2,444 $\mu A\ mM^{-1}\ cm^{-2}$ and a detection limit of 76.9 nM (*S/N* = 3) were found for the Cu_2O electrode. In the case of $Cu_2O@Cu_{1.8}S$ electrode, a sensitivity of 3,630 $\mu A\ mM^{-1}\ cm^{-2}$ was found, a much higher value than that of Cu_2O, with a lower detection limit of 67.8 nM (*S/N* = 3). For comparison purposes, the performances of other copper oxide-based glucose sensors reported in literature are listed in Table 1. It can be seen that the sensor based on $Cu_2O@Cu_{1.8}S$ exhibits better sensing performances in terms of sensitivity, detection potential and linear range than some of copper oxide/copper sulfide-based sensors [18, 35, 36], implying that the $Cu_2O@Cu_{1.8}S$ material can be a promising and effective electrode for non-enzymatic glucose sensing. It is worth noting that the reported CuO film [34] and CuS modified Cu

14

electrodes [37] also showed an improved linearity and sensitivity to glucose compared to our Cu_2O and $Cu_2O@Cu_{1.8}S$ modified electrodes, which could be possibly attributed to an improved electronic conductivity. This finding suggests that there is still some room for further improvement in performances for $Cu_2O@Cu_{1.8}S$ by using highly conductive support materials.

Electrode	Sensitivity/ $\mu A\ cm^{-2}\ mM^{-1}$	Linear Range/ mM	DoL / μM	Reference
$Cu_2O@Cu_{1.8}S$	3630	0.001-1	0.0678	herein
Cu_2O	2444	1-0.8	0.0769	herein
Cu/Cu_2O	1434	0-40	1.6	[35]
Cu_2O spindle	2828	0.001-1	0.3	[18]
Dandelion-like CuO films	5368	0.005-1.6	1.2	[34]
CuO nanoparticles	2762.5	0.05-18.45	0.5	[36]
$Cu_2S@Cu$	11750.8	0.0002-0.63	0.07	[37]
CuS nanotubes	7.842	0.05-5	10	[38]
$Cu_2SNP(EN)/GC$	61.67	0.01-3.1	1.3	[39]

Table 1. Comparison of the key performance characteristics of some existing CuO-based electrodes for non-enzymatic electrooxidation of glucose.
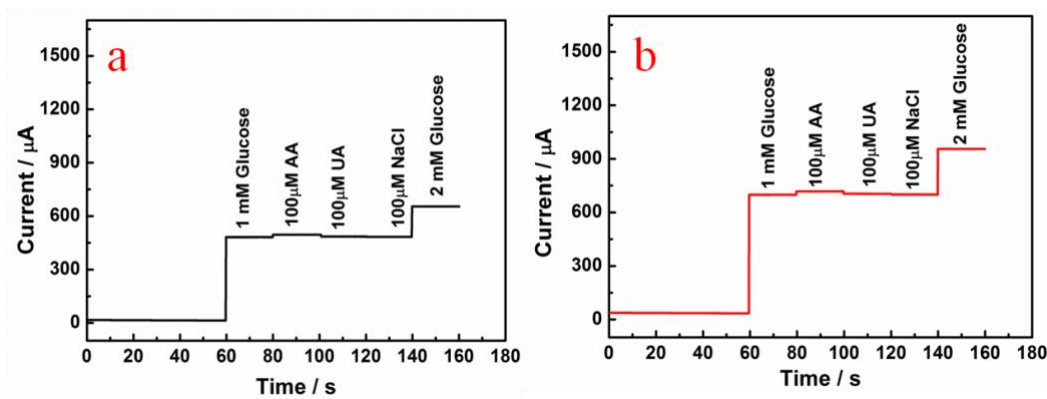
Figure 6. Amperometric responses of the Cu_2O and $Cu_2O@Cu_{1.8}S$ electrodes with continuous injections of 1.0 mM glucose and 0.1 mM interferents of AA, UA, and NaCl into 0.1 M NaOH at a potential of +0.50 V vs. Ag/AgCl.

It is known that some easily oxidative species, such as ascorbic acid (AA), uric acid (UA), NaCl and other carbohydrate compounds, usually co-exist with glucose in biological samples and consequently may interfere with the detection of glucose. Therefore, selectivity is an important factor for the practical use of glucose sensors.

According to previous works, a normal physiological level of glucose is 3 – 8 mM, which is at least 10 times higher than that of the interfering species. The amperometric responses of the two electrodes by stepwise addition of 1.0 mM glucose in the presence of 0.1 mM of various interfering species at an applied potential of +0.50 V vs. Ag/AgCl is shown in Figure 6. From the figure, an obvious response of glucose oxidation can be observed, but there was no obvious current response from the interfering species, indicating that, in our conditions, a high selectivity against most of the important interfering species can be achieved with the Cu_2O and $Cu_2O@Cu_{1.8}S$ electrodes in an alkaline media. The excellent anti-interference

16

property of Cu_2O and $Cu_2O@Cu_{1.8}S$ electrodes for glucose against interfering species could be mainly ascribed to the intrinsic property of Cu_2O, as well as its unique nanostructure. Under an alkaline environment (0.1 M NaOH), the surface of Cu_2O and $Cu_2O@Cu_{1.8}S$ may be negatively charged based on the value of isoelectric point for Cu_2O (9.5); Moreover, interfering species like UA and AA may also be negatively charged due to the deprotonated effect in alkaline solution [18, 34, 36, 40, 41]. Consequently, the negatively charged UA and AA could be repelled on the negatively charged surface of Cu_2O and $Cu_2O@Cu_{1.8}S$, thus resulting in corresponding weak signals.

4. Conclusions

The authors demonstrated for the first time the use of $Cu_2O@Cu_{1.8}S$ as a posssible electrode material toward non-enzymatic glucose detection. $Cu_2O@Cu_{1.8}S$ hybrid materials were successfully prepared by an in-situ growth method, in which out-diffusion of spherical Cu_2O templates led to a hollow structure. Electrochemical measurements showed that $Cu_2O@Cu_{1.8}S$ exhibited a better electrocatalytic activity toward glucose oxidation than Cu_2O, which was attributed to the synergetic effects between Cu_2O and $Cu_{1.8}S$. The as-prepared $Cu_2O@Cu_{1.8}S$ sensor exhibited a rapid response of 5 s, a wide linear range in glucose concentrations of 0.001–1mM, a high selectivity of 3630 $\mu A\ mM^{-1}\ cm^{-2}$, and a low detection limit of 67.8 nM. Moreover, the sensor exhibited relatively excellent selectivity in 'real' sample analysis. The excellent sensing performances make $Cu_2O@Cu_{1.8}S$ a promising candidate in the

development of non-enzymatic glucose sensors.

Acknowledgements

Reference

[1] R.M. Tehrani, S. Ab Ghani, MWCNT-ruthenium oxide composite paste electrode as non-enzymatic glucose sensor, Biosens. Bioelectron. , 38 (2012) 278-283.

[2] C.L. Jr, C. Lyons, Electrode systems for continuous monitoring in cardiovascular surgery, Ann. N.Y. Acad. Sci. , 102 (1962) 29–45.

[3] R. Wilson, A.P.F. Turner, Glucose oxidase: an ideal enzyme, Biosensors & Bioelectronics, 7 (1992) 165-185.

[4] J.X. Wang, X.W. Sun, A. Wei, Y. Lei, X.P. Cai, C.M. Li, Z.L. Dong, Zinc oxide nanocomb biosensor for glucose detection, Appl. Phys. Lett. , 88 (2006) 34.

[5] C. Malitesta, F. Palmisano, L. Torsi, P.G. Zambonin, Glucose fast-response amperometric sensor based on glucose oxidase immobilised in an electropolymerized poly(o -phenylenediamine) film. Anal Chem 62: 2735-2740, 62 (1991) 2735-2740.

[6] J. Wang, D.F. Thomas, A. Chen, Nonenzymatic Electrochemical Glucose Sensor
Based on Nanoporous PtPb Networks, Anal. Chem., 80 (2008) 997-1004.

[7] F. Xiao, F. Zhao, D. Mei, Z. Mo, B. Zeng, Nonenzymatic glucose sensor based on ultrasonic-electrodeposition of bimetallic PtM (M=Ru, Pd and Au) nanoparticles on carbon nanotubes-ionic liquid composite film, Biosens. Bioelectron. , 24 (2009) 3481-3486.

[8] A. Liu, Q. Ren, T. Xu, M. Yuan, W. Tang, Morphology-controllable gold nanostructures on phosphorus doped diamond-like carbon surfaces and their electrocatalysis for glucose oxidation, "Sens. Actuators, B ", 162 (2012) 135-142.

[9] J.-J. Yu, S. Lu, J.-W. Li, F.-Q. Zhao, B.-Z. Zeng, Characterization of gold nanoparticles electrochemically deposited on amine-functioned mesoporous silica films and electrocatalytic oxidation of glucose, J. Solid State Electrochem. , 11 (2007) 1211-1219.

[10] V. Veeramani, R. Madhu, S.-M. Chen, P. Veerakumar, C.-T. Hung, S.-B. Liu, Heteroatom-enriched porous carbon/nickel oxide nanocomposites as enzyme-free highly sensitive sensors for detection of glucose, "Sens. Actuators, B ", 221 (2015) 1384-1390.

[11] K. Singh, A. Umar, A. Kumar, G.R. Chaudhary, S. Singh, S.K. Mehta, Non-Enzymatic Glucose Sensor Based on Well-Crystallized ZnO Nanoparticles, Science of Advanced Materials, 4 (2012) 994-1000.

[12] Q. Yi, F. Niu, W. Yu, Pd-modified TiO2 electrode for electrochemical oxidation of hydrazine, formaldehyde and glucose, Thin Solid Films 519 (2011) 3155-3161.

[13] S. Felix, B.P. Chakkravarthy, S.K. Jeong, A.N. Grace, Synthesis of Pt Decorated Copper Oxide Nanoleaves and Its Electrochemical Detection of Glucose, J. Electrochem. Soc., 162 (2015) H392-H396.

[14] S. Harish, M. Navaneethan, J. Archana, S. Ponnusamy, C. Muthamizhchelvan, Y. Hayakawa,

Controlled synthesis and morphological investigation of self-assembled CuO nanostructures, Mater. Lett. , 121 (2014) 129-132.

[15] D.P. Singh, A.K. Ojha, O.N. Srivastava, Synthesis of Different Cu(OH)2 and CuO (Nanowires, Rectangles, Seed-, Belt-, and

Sheetlike) Nanostructures by Simple Wet Chemical Route, J. Phys. Chem. C, 113 (2009) 3409-3418.

[16] S. He, J. Li, J. Wang, G. Yang, Z. Qiao, Facile synthesis and lithium storage performance of hollow CuO microspheres, Mater. Lett. , 129 (2014) 5-7.

[17] X. Ma, Q. Zhao, H. Wang, S. Ji, Controlled Synthesis of CuO from needle to flower-like Particle Morphologies for Highly Sensitive Glucose Detection, Int. J. Electrochem. Sci. , 12 (2017) 8217-8226.

[18] Y. Liu, Q. Zhao, J. Ding, H. Wang, Y. Ma, W. Lv, S. Ji, S. Li, R. Wang, Synthesis of hierarchical three-dimensional CuO spindles for highly sensitive glucose determination,   Micro & Nano Letters, Institution of Engineering and Technology, 2016, pp. 870-875.

[19] D. Ye, G. Liang, H. Li, J. Luo, S. Zhang, H. Chen, J. Kong, A novel nonenzymatic sensor based on CuO nanoneedle/graphene/carbon nanofiber modified electrode for probing glucose in saliva, Talanta, 116 (2013) 223-230.

[20] X. Wang, C. Hu, H. Liu, G. Du, X. He, Y. Xi, Synthesis of CuO nanostructures and their application for nonenzymatic glucose sensing, "Sens. Actuators, B ", 144 (2010) 220-225.

[21] M.-J. Song, S.-K. Lee, J.-H. Kim, D.-S. Lim, Non-Enzymatic Glucose Sensor Based on Cu Electrode Modified with CuO Nanoflowers, J. Electrochem. Soc., 160 (2013) B43-B46.

[22] X. Yan, J. Yang, L. Ma, X. Tong, Y. Wang, G. Jin, X.-Y. Guo, Size-controlled synthesis of Cu2O nanoparticles on reduced graphene oxide sheets and their application as non-enzymatic glucose sensor materials, J. Solid State Electrochem. , 19 (2015) 3195-3199.

[23] Y. Tian, Y. Liu, W.-p. Wang, X. Zhang, W. Peng, CuO nanoparticles on sulfur-doped graphene for nonenzymatic glucose sensing, Electrochim. Acta, 156 (2015) 244-251.

[24] C. Karuppiah, M. Velmurugan, S.-M. Chen, S.-H. Tsai, B.-S. Lou, M. Ajmal Ali, F.M.A. Al-Hemaid, A simple hydrothermal synthesis and fabrication of zinc oxide–copper oxide heterostructure for the sensitive determination of nonenzymatic glucose biosensor, "Sens. Actuators, B ", 221 (2015) 1299-1306.

[25] D. Li, Y. He, S. Wang, On the Rotation of the Janus CuO/CuS Colloids Formed at a Pickering Emulsion Interface, J.phys.chem.c, 113 (2009) 12927-12929.

[26] H. Zhu, J. Wang, D. Wu, Fast synthesis, formation mechanism, and control of shell thickness of CuS hollow spheres, Inorg. Chem. , 48 (2009) 7099.

[27] D. Tahir, S. Tougaard, Electronic and optical properties of Cu, CuO and Cu2O studied by electron spectroscopy, Journal of Physics Condensed Matter An Institute of Physics Journal, 24 (2012) 175002.

[28] Z. Li, Z. Zhang, Tetrafunctional Cu 2 S thin layers on Cu 2 O nanowires for efficient photoelectrochemical water splitting, Nano Research, (2017) 1-11.

[29] H. Zou, T. Yang, J. Lan, C. Huang, Use of the peroxidase mimetic activity of erythrocyte-like Cu1.8S nanoparticles in the colorimetric determination of glutathione, Anal. Methods 9(2017) 841-846.

[30] Y. Ma, H. Wang, K. Julian, S. Ji, W. Lv, R. Wang, Control of CuO nanocrystal morphology from ultrathin "willow-leaf"to "flower-shaped" for increased hydrazine oxidation activity, J. Power Sources, 300 (2015) 344-350.

[31] Y. Ma, H. Li, R. Wang, H. Wang, W. Lv, S. Ji, Ultrathin willow-like CuO nanoflakes as an efficient catalyst for electro-oxidation of hydrazine, J. Power Sources, 289 (2015) 22-25.

[32] L. Wang, H. Wang, Synthesis of shuttle-shaped porous CuO in water microdroplets for increased

hydrazine oxidation, Micro & Nano Letters, (2017).

[33] S. Sun, X. Zhang, Y. Sun, J. Zhang, S. Yang, X. Song, Z. Yang, A facile strategy for the synthesis of hierarchical CuO nanourchins and their application as non-enzymatic glucose sensors, RSC Advances, 3 (2013) 13712-13719.

[34] K. Li, G. Fan, L. Yang, F. Li, Novel ultrasensitive non-enzymatic glucose sensors based on controlled flower-like CuO hierarchical films, "Sens. Actuators, B ", 199 (2014) 175-182.

[35] X. Cheng, J. Zhang, H. Chang, L. Luo, F. Nie, X. Feng, High performance Cu/Cu2O nanohybrid electrocatalyst for nonenzymatic glucose detection, Journal of Materials Chemistry B, 4 (2016).

[36] R. Ahmad, M. Vaseem, N. Tripathy, Y.-B. Hahn, Wide Linear-Range Detecting Nonenzymatic Glucose Biosensor Based on CuO Nanoparticles Inkjet-Printed on Electrodes, Anal. Chem., 85 (2013) 10448-10454.

[37] W. Lu, Y. Sun, H. Dai, P. Ni, S. Jiang, Y. Wang, Z. Li, Z. Li, Fabrication of cuprous sulfide nanorods supported on copper foam for nonenzymatic amperometric determination of glucose and hydrogen peroxide, RSC Advances, 6 (2016) 90732-90738.

[38] X. Zhang, G. Wang, A. Gu, Y. Wei, B. Fang, CuS nanotubes for ultrasensitive nonenzymatic glucose sensors, Chem. Commun. , 45 (2008) 5945-5947.

[39] S.K. Maji, A.K. Dutta, G.R. Bhadu, P. Paul, A. Mondal, B. Adhikary, A novel amperometric biosensor for hydrogen peroxide and glucose based on cuprous sulfide nanoplates, Journal of Materials Chemistry B, 1 (2013) 4127-4134.

[40] F. Huang, Y. Zhong, J. Chen, S. Li, Y. Li, F. Wang, S. Feng, Nonenzymatic glucose sensor based on three different CuO nanomaterials, Anal. Methods 5(2013) 3050.

[41] S. Sun, X. Zhang, Y. Sun, S. Yang, X. Song, Z. Yang, Facile water-assisted synthesis of cupric oxide nanourchins and their application as nonenzymatic glucose biosensor, ACS Appl. Mater. Interfaces 5(2013) 4429-4437.